RESEARCH ARTICLE





High throughput solubility and redissolution screening for antibody purification via combined PEG and zinc chloride precipitation

Qin Gu¹ | Zhao Li² | Jonathan L. Coffman³ | Todd M. Przybycien^{1,4} | Andrew L. Zydney² |

Correspondence

Todd M. Przybycien, Department of Chemical and Biological Engineering, Rensselaer Polytechnic Institute, Troy, NY 12180. Email: przybt3@rpi.edu

Funding information

Carnegie Mellon University, Department of Chemical Engineering; National Science Foundation, Grant/Award Number: CBET 1705642; PPG Industries

Abstract

As upstream product titers increase, the downstream chromatographic capture step has become a significant "downstream bottleneck." Precipitation becomes more attractive under these conditions as the supersaturation driving force increases with the ever-increasing titer. In this study, two precipitating reagents with orthogonal mechanisms, polyethylene glycol (PEG) as a volume excluder and zinc chloride (ZnCl₂) as a cross linker, were examined as precipitants for two monoclonal antibodies (mAbs), one stable and the other aggregation-prone, in purified drug substance and harvested cell culture fluid forms. Manual batch solubility and redissolution experiments were performed as scouting experiments. A high throughput (HTP) liquid handling system was used to investigate the design space as fully as possible while reducing time, labor, and material requirements. Precipitation and redissolution were studied by systematically varying the concentrations of PEG and ZnCl₂ to identify combinations that resulted in high yield and good quality for the stable mAb; PEG concentrations in the range 7-7.5 wt/vol% together with 10 mM ZnCl₂ gave a yield of 97% and monomer contents of about 93%. While yield for the unstable mAb was high, quality was not acceptable. Performance at selected conditions was further corroborated for the stable mAb using a continuous tubular precipitation reactor at the laboratory scale. The HTP automation system was a powerful tool for locating desired (customized) conditions for antibodies of different physicochemical properties.

KEYWORDS

bioseparations, capture step, monoclonal antibody, protein precipitation, protein solubility

1 | INTRODUCTION

In an effort to increase monoclonal antibody (mAb) manufacturing process throughput and reduce costs, the biomanufacturing industry has achieved upstream titers on the order of 5 g/L and above by high-productivity cell line selection, growth media optimization, and bioreactor engineering.¹ As a result, the manufacturing bottleneck has shifted toward downstream processes, which can constitute up to 80% of total manufacturing costs.²⁻⁴ For example, the performance of the capture

step of the platform mAb purification process, protein A chromatography, has been challenged by the high titers achieved in the upstream process.⁵ As mAb titer increases, higher binding capacity, hence higher protein A ligand densities, and larger column volumes, are required to accommodate the additional antibody molecules, adding to the operating costs via increased media costs. Further, higher titers result in more viscous process streams, leading to larger pressure drops and less efficient mass transfer within the column, both of which complicate column operation. Dilution of the inlet stream before a protein A capture step is

¹Department of Chemical Engineering, Carnegie Mellon University, Pittsburgh, Pennsylvania

²Department of Chemical Engineering, The Pennsylvania State University, State College, Pennsylvania

³Process Science, Boehringer Ingelheim Pharmaceuticals Inc., Fremont, California

⁴Department of Chemical and Biological Engineering, Rensselaer Polytechnic Institute, Troy, New York

an option, but the added volume would require either additional chromatography runs or larger column volumes and defeats much of the purpose of achieving higher titers in the first place.

As the titer of recombinant protein drugs starts to approach the typical concentrations of the major plasma proteins, for example, albumin at 35-45 g/L and gamma globulins at 7-15 g/L⁶, it makes sense to consider some of the purification tools that have been developed for the plasma fractionation industry, in particular target precipitation.⁷ Indeed, target protein capture via precipitation has generated increased interest over the past few years as an attractive alternative to conventional chromatographic capture.⁸⁻¹² In target precipitation, higher titers translate to larger supersaturations, which is defined as the ratio of the target concentration before precipitation to the equilibrium solubility or steady-state concentration afterward, leading to increased yields for given precipitation conditions. Further, in the target precipitation scenario, since the target is less soluble than the impurities, the purity will also increase with higher titers and the associated higher precipitate yields. Other bulk separation techniques. such as crystallization¹³ and aqueous two-phase extraction¹⁴ also become more attractive under these conditions.

Precipitation occurs when solution conditions or the surface chemistry of proteins are altered in some way, for example, by the change of temperature, pH, or dielectric constant, or by addition of salts, polymers, or cross-linking species. ^{15,16} It is important that the precipitants be nondenaturing and reversible toward the target proteins, so that the recovered product retains activity. Precipitates can be generated in simple equipment, such as stirred tanks or tubular reactors with static inline mixers, using either batch or continuous formats. ^{15,16} Precipitate slurries are dewatered by passage through a solid/liquid separator, such as a centrifuge or a filter, to remove the supernatant and capture the target protein in a concentrated slurry form. This concentrated slurry can then be washed to further remove residual supernatant and adsorbed impurities. Finally, the washed precipitate is redissolved to recover purified protein.

Among possible precipitants and precipitant combinations, the addition of nonionic polymers and metal ions stands out because they are relatively inexpensive, effective at low dosage, form reversible precipitate solids that are easy to redissolve and do not denature the protein during precipitation and redissolution. Polyethylene glycol (PEG) induced protein precipitation has been studied extensively and the general consensus is that the protein solubility follows a log-linear behavior with respect to the concentration of PEG. ¹⁷⁻¹⁹ Divalent zinc cations are very effective as reversible protein cross-linkers at low concentration compared with cobalt, copper, and other multivalent transition metal cations. ^{20,21} More importantly, using both reagents together can result in a synergistic rather than additive effect on lowering protein solubility. This means low concentrations of PEG and ZnCl₂ combined can achieve high precipitation yields. ^{22,23}

However, it can be challenging to identify the desirable concentrations of PEG and ZnCl₂ for the precipitation of mAb products. Previously, batch experiments were used to determine protein solubility with respect to individual precipitants. ¹⁸ These experiments are easy to set up, but require at least a few grams of mAb product to cover a

wide range of precipitant concentrations. Conversely, high throughput (HTP) methods in a 96-well plate format using programmable robotic liquid handling systems are gaining popularity in studying precipitation and crystallization. ²⁴⁻²⁶ Knevelman et al. ²⁷ used HTP experimentation to explore more than 1,000 conditions with less than 1 g of mAb for PEG-based precipitation of an IgG4 mAb. In fact, the application of HTP methods early on during process development for biopharmaceuticals is more common in both upstream and downstream sections due to the pressure to optimize the manufacturing process as early as possible to ensure rapid clinical entry and an accelerated pathway to licensure. ²⁸ The ability to carry out many miniature experiments in parallel enables exploration of an expanded design space in a controlled and consistent manner using only milliliter or microliter volumes of high-value molecule solutions.

Moreover, it is critical to locate the optimal operating region for precipitation early on in process development. Because the concentration of target therapeutics in the inlet stream for the capture step is typically not constant due to variations between batches or different growth phases in a continuous perfusion bioreactor, the design space that needs to be explored must also consider the variation in product titer. Exploiting a HTP method early on can build the database needed for design, control, and optimization of scaled-up pilot and commercial processes.

In this work, we explored the use of a HTP method to determine the solubility, precipitation, and redissolution behaviors of two monoclonal antibodies (mAb) in HEPES buffer and in their respective harvested cell culture fluid (HCCF) by systematically varying PEG and zinc chloride concentrations in a combined precipitation method. The objective was to narrow down the appropriate precipitation conditions for subsequent exploration in an integrated continuous precipitation-filtration reactor system.²⁹ Because continuous processes can consume a great deal of target material at even small laboratory scales, precipitant scoping studies using a continuous format are impractical. We also determined postprecipitation impurity contents in terms of low and high molecular weight species for selected conditions that provided high mAb yield from harvested cell culture fluids (HCCF). This was done to address concerns that precipitation could decrease product quality by increasing aggregate levels and as a point of performance comparison with the typical capture processes via protein A chromatography. Batch, HTP, and continuous precipitation formats gave consistent mAb solubility behaviors based on yield and overall performance metrics.

2 | MATERIALS AND METHODS

2.1 | Materials

We investigated two mAbs, both in purified drug substance (DS) and HCCF forms, provided by Boehringer Ingelheim Pharmaceuticals, Inc. (Fremont, CA). These mAbs were expressed in different CHO host cell lines, therefore the impurity profiles in the HCCFs were different. In addition, the two mAbs have different isoelectric points (pl); specific values cannot be disclosed. Cedex BioHT (Roche CustomBiotech, Indianapolis, IN) analyses of the total protein and IgG content of the

3 of 14

HCCFs prior to precipitation indicated that the mAbs accounted for about 50% or less of the total protein.

PEG of molecular weight 3,350 g/mol (88276), 100 mM ZnCl₂ solution (39059), and 1 M HEPES buffer (H3537) were purchased from MilliporeSigma (St. Louis, MO). Nunc™ 96 DeepWell™ plates (Z717274), MultiScreenHTS GV filter plates with 0.22 μm PVDF membranes (MSGVS2210), and Greiner UV-Star® 96 well plates (M3812) were also purchased from MilliporeSigma. MicroAmp™ Optical Adhesive (4313663) was purchased from Thermo Fisher Scientific (Waltham, MA). All solutions were prepared with deionized water with a resistivity greater than or equal to 18 mΩ·cm and were sterile filtered using Millipore SteriCup® Filters with 0.22 μm PES membranes (SCGPU11RE) obtained from MilliporeSigma (Burlington, MA).

2.2 | Buffer and stock solutions preparation

All mAb DS precipitations were conducted in 4-(2-hydroxyethyl)-1-piperazineethanesulfonic acid (HEPES) buffer. HEPES buffer was chosen because of its buffering capacity near neutral pH and its negligible complexation of Zn²⁺ ions in solution, which should minimize the formation of zinc hydroxychloride complexes that could deplete Zn²⁺ before mAb precipitation.³⁰ Other buffers, such as 3-morpholinopropane-1-sulfonic acid (MOPS) also fit these criteria but were not chosen as HEPES was already used in later polishing steps in existing platform downstream processes for these mAbs. We note that other common neutral pH buffers, such as tris and phosphate, are particularly poor choices due to extensive complexation with divalent metal cations.

To make 50 mM HEPES buffer at pH 7, 1 M HEPES stock solution was diluted with DI water to 80% of the final volume. The pH of the diluted HEPES solution was adjusted to 7 by adding 1 M NaOH and then brought to the final volume and sterile filtered. The final buffer solutions were stored at room temperature. All stock solutions of PEG-3350 and ZnCl₂ were made with 50 mM HEPES buffer, pH 7.

Similarly, 100 mM acetate buffer, pH 5 was prepared by dissolving appropriate amounts of sodium acetate and acetic acid; this was used as a redissolution buffer for both mAbs.

Stock solutions of 50 wt/vol% PEG-3350 were made by dissolving appropriate amounts of PEG-3350 powder in 50 mM HEPES buffer. Zinc chloride solutions of desired concentration were made by direct dilution of the commercial 100 mM stock solution with HEPES buffer immediately before each experiment to minimize the formation of insoluble zinc hydroxychloride complexes.

2.3 | Monoclonal antibody solutions

Antibodies in DS form, generated by pooling product from previous downstream pilot plant runs, were buffer exchanged by diafiltration with eight diavolumes of the HEPES buffer using a 30 kDa Amicon® Ultra-15 Centrifugal Filter Unit. The resulting concentration for the mAb-1 pool "stock" was 102 g/L; the mAb-2 pool 'stock' was 58 g/L.

These solutions were used as is or diluted with HEPES buffer to the desired concentration.

Antibodies in HCCF were collected from 2 L perfusion bioreactors at peak growth phase. The mAb-1 titer was 2.8 g/L and was used as is or concentrated by ultrafiltration through 30 kDa Amicon filters. The mAb-2 HCCF titer was 1.5 g/L and was concentrated using Pall Cadence single pass tangential flow filtration (SPTFF) modules with nine stages having 30 kDa PES membranes to achieve a mAb concentration of 22.8 g/L, a roughly 15-fold concentration factor. This mAb-2 HCCF "stock" was further diluted with HEPES buffer or filtrate from the SPTFF step to the desired concentrations for batch and HTP solubility experiments. Due to the differing solubility results obtained using HEPES or SPTFF filtrate, three different dilution buffers were investigated and compared: original filtrate at pH 8, original filtrate pH-adjusted to 7, and HEPES buffer at pH 7.

2.4 | Batch precipitation and redissolution experiments

Batch solubility experiments using PEG-3350 and ZnCl₂ were performed to determine the concentration range of PEG and ZnCl2 to use in subsequent HTP experiments. A range of PEG and ZnCl₂ concentrations were prepared by combining different volumes of 50 wt/ vol% PEG stock or 40 mM ZnCl₂ stock, respectively, and HEPES buffer. Precipitations were initiated by mixing equal volumes of protein and precipitant solutions at double the targeted species concentrations to compensate for the twofold dilution on mixing. All mAb titers and precipitant concentrations reported in the context of solubility determinations refer to concentrations after mixing. Here. 600 µl of the mAb solution was added into each microcentrifuge tube followed by addition of 600 µl PEG or ZnCl₂ stock. Solutions were mixed by repeated gentle pipetting. The resulting mixtures were incubated at room temperature for at least 4 hr before centrifuging at 8,000 rpm for 20 min using an Eppendorf bench-top centrifuge. If the supernatant was not clear, additional centrifugation in increments of 10 min was used until a clear supernatant was obtained as determined by visual inspection. Samples of the supernatant, typically 100-150 μl, were drawn for absorbance measurements at 280 nm using variable path-length spectroscopy with a SoloVPE system connected to an Agilent® Cary 60 spectrophotometer. Concentrations were calculated from the Beer-Lambert Law using the path length determined by the SoloVPE system and the corresponding known extinction coefficients for both mAbs.

Precipitate redissolution was accomplished by decanting the supernatant from the pellet, gently withdrawing any residual with a pipette, and then adding 1,000 μl of acetate buffer. Pellets were disrupted by gentle pipetting. After 4 hr of incubation at room temperature, the solutions were clear. Nonetheless, the redissolution mixtures were centrifuged at 8,000 rpm for 20 min to settle any undissolved particulate matter. Samples of the redissolved solution, typically 100–150 μl , were drawn for mAb concentration determination using the SoloVPE system as described earlier.

2.5 | HTP precipitation and redissolution experiments

The HTP workstation used was a Tecan Freedom Evo® 200 robot equipped with a Liquid Handling (LiHa) arm of fixed steel tips, an Extended Robotic Manipulator (RoMA) arm, and a Te-Shake™ orbital shaker with two slots for well plates. The plate reader was a Tecan Infinite® M200 Pro Nano Quant with a Hettich ROTANTA 460 Robotics centrifuge mounted at the bottom of the workstation. The system was controlled using the Freedom Evoware® software. A schematic of the workstation is shown in Figure 1 where the fixed steel tips are connected to water for cleaning and liquid displacement using syringe pumps and controlled by commands in Evoware® before each run.

For precipitation screening experiments, first, a "buffer plate" was created by pipetting different amounts of HEPES buffer, $ZnCl_2$ and PEG stock solutions, in this order, from respective reagent troughs into 8×8 wells in a 96-well DeepWell plate according to a worksheet. This worksheet was precalculated so that there was a gradient in $ZnCl_2$ concentration across the columns and a gradient in PEG concentration down the rows of the plate as shown in Figure 2. The total volume of reagents in each well was 1,000 μ l. Mixing of the PEG and $ZnCl_2$ solutions was achieved by gentle aspiration right after dispensing the PEG solutions. This mixing prevented the denser and more viscous PEG stock solutions from settling to the bottom of the well as a separate layer. Note that for solutions containing PEG or

precipitate solids, the "viscous dispense" method was chosen in the software, while all other dispense methods were set to "water free dispense."

Second, $500 \,\mu l$ of mAb solution (either purified DS in HEPES buffer or HCCF) was pipetted into each well of a DeepWell ® "reaction plate" followed by addition of 500 µl of PEG/ZnCl₂ solution from the corresponding well of the buffer plate and then gentle mixing by aspiration. Note again the twofold dilution of both protein and precipitants in this precipitation protocol. As above, all mAb titers and precipitant concentrations reported in the context of solubility determinations refer to concentrations after mixing the protein and precipitants. The reaction plate was then sealed by hand and moved with the RoMA to the orbital shaker for incubation at room temperature for 2 hr at 900 rpm. After incubation, the reaction plate was returned to the plate holder and the seal was removed. The precipitation mixture in each well was mixed by aspiration to ensure even distribution of solids. Then 200 µl of the mixture was transferred to the filter plate. This filter plate was placed on top of UV Plate 1 in the Hettich centrifuge for 30 min at 800 rpm to achieve solid-liquid separation. For purified mAbs precipitated in HEPES buffer, the collected liquid fraction in UV Plate 1 was read for volume and concentration. For mAbs precipitated in HCCF, the collected liquid fraction in UV Plate 1 was read only for volume. After centrifuging the reaction plate for 30 min at 800 rpm, the mAb concentration in the supernatant was instead measured manually using a Cedex BioHT analyzer as explained later in this section.

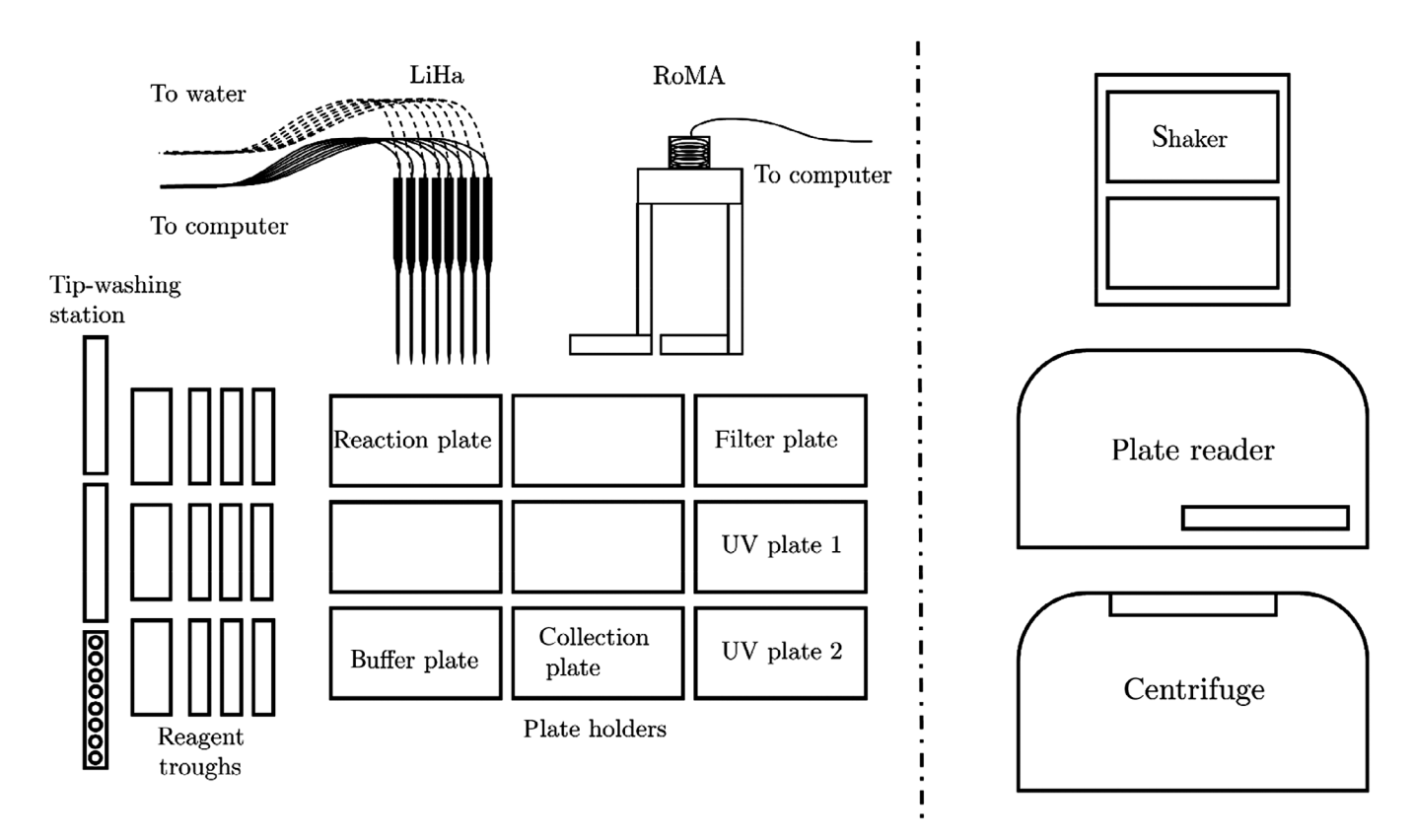
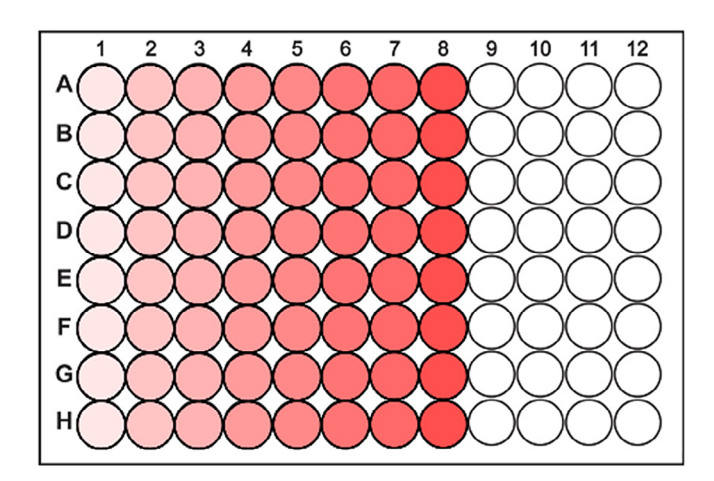


FIGURE 1 Schematic of Tecan® Evo200 workstation



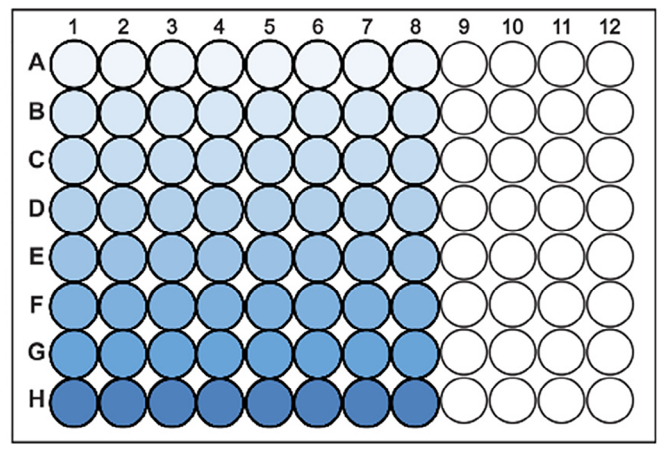


FIGURE 2 Left: concentration gradient of $ZnCl_2$ across the columns. Right: concentration gradient of PEG down the rows. Darker colors represent higher concentrations. Actual plates have gradients in both $ZnCl_2$ (red) and PEG (blue) in the same 96-well plate. PEG, polyethylene glycol

For redissolution measurements, 200 μ l of acetate buffer was added to the same filter plate carrying the precipitated protein, and other impurities in the case of HCCF, before being placed on top of the collection plate on the shaker. The filter plate was then sealed by hand and incubated for 2 hr at 900 rpm to redissolve the precipitated protein. The use of a collection plate instead of a UV plate on the orbital shaker avoided scratches on the bottom of the UV plate.

Similarly, after incubation, the filter plate was unsealed and then put on top of UV Plate 2 in the centrifuge for 30 min at 800 rpm to collect redissolved mAbs. UV Plate 2 was also put into the plate reader for volume and concentration measurements.

2.6 | Volume and concentration determination in HTP experiments

For mAb from purified DS in HEPES or acetate buffer, the path length of liquid in each well was determined using a method similar to that described in Knevelman et al²⁷. In this study, due to instrument limitations, absorbance was measured at 977 nm (instead of 1,000 nm) and at 900 nm.

The path length was calculated with the following equation using absorbance measurements of water in a 1 cm cuvette as a standard:

$$\frac{(\mathsf{A977}\!-\!\mathsf{A900})_{\mathsf{sample}\,\mathsf{in}\,\mathsf{well}}}{(\mathsf{A977}\!-\!\mathsf{A900})_{\mathsf{water}\,\mathsf{in}\,\mathsf{1}\,\mathsf{cm}\,\mathsf{cuvette}}} = \mathsf{pathlength}\,(\mathsf{cm}) \tag{1}$$

Similarly, the volume of liquid in each well was calculated using the following equation:

$$\frac{(A977-A900)_{sample\;in\;well}}{(A977-A900)_{200\;\mu L\;water\;in\;well}} \times 200\;\mu l = volume\;of\;sample\;(\mu l) \qquad (2)$$

The concentration of mAb in each well can then be obtained based on the calculated path length, the known extinction coefficient,

and the measured absorbance at 280 nm using the Beer–Lambert Law, where A is the absorbance, ε is the extinction coefficient, C is the concentration, and I is the path length:

$$A = \varepsilon C I \tag{3}$$

For mAb in HCCF, the concentration of mAb in the supernatant was determined using a Cedex BioHT analyzer with accompanying IgG (human) assay kits. For each sample, $300\text{--}500\,\mu\text{l}$ was used for measurements. This assay uses an immunoturbidimetric technique where a specific antiserum binds with human IgG present in the sample and the evolving absorbance is measured at 340 nm³1.

2.7 | Assay for impurities

Size exclusion chromatography (SEC) was used for this assay. The unsettled precipitation mixture was dewatered by filtration through 0.2 μm microcentrifuge filters at 800 rpm for 30 min using a benchtop centrifuge. The flow-through supernatant was discarded, 500 μl of 100 mM acetate buffer at pH 5 was added to the retained, wet precipitate, and the filter tube was incubated for 2 hr at room temperature. The redissolved solution was then mixed with SEC running buffer in a 1:1 ratio and centrifuged to remove any particulates. The impurities, including mAb fragments and aggregates, were determined using in-house SEC protocols for the corresponding mAbs.

3 | RESULTS AND DISCUSSION

Three stages of screening experiments were performed. The first comprised manual, small-scale batch experiments with mAb-1 and mAb-2 DS pool materials in HEPES buffer using only PEG or $\rm ZnCl_2$ to roughly scope out the effective precipitant concentration ranges as a function of mAb concentration and simplify supernatant analyses for

residual mAb. The second was also manual, using small-scale batch precipitations of mAb-1 and mAb-2 in HCCF with PEG and $ZnCl_2$ separately and combined to identify any synergistic effects of PEG and $ZnCl_2$ and to understand the impact of contaminant species on mAb precipitation yields. The last screen used a HTP precipitation and redissolution format for both mAbs in HCCF and with PEG and $ZnCl_2$ combined to identify optimal solution conditions. The PEG and $ZnCl_2$ concentrations, which resulted in high precipitation yields in each stage were used to focus the concentration ranges examined in the next stage.

3.1 | Batch precipitation of mAb DS pool materials in HEPES

Table 1 summarizes the mAb titers and the PEG and $ZnCl_2$ concentration ranges investigated in the first stage. The three titers were chosen to represent current and future upstream productivities and to investigate the impact of preconcentration.

The mechanism of PEG-induced protein precipitation is volume exclusion/solution depletion. The corresponding theory provides the protein solubility as a log-linear function of the PEG concentration. The intercept represents an extrapolated intrinsic protein solubility. The slope depends on the hydrodynamic radius of both the protein and PEG molecules, with more negative slopes and higher precipitation effectiveness corresponding to larger molecules. In our study, PEG with a nominal molecular weight of 3,350 g/mol was chosen over other commonly available molecular weights as a compromise between precipitation effectiveness and impact on solution viscosity. The slope depends on the hydrodynamic radius of both the protein and PEG molecules, with more negative slopes and higher precipitation effectiveness and impact on solution viscosity. The slope depends on the hydrodynamic radius of both the protein and PEG molecules, with more negative slopes and higher precipitation effectiveness and impact on solution viscosity. The slope depends on the hydrodynamic radius of both the protein and PEG molecules, with more negative slopes and higher precipitation effectiveness and higher precipitation effectiveness and impact on solution viscosity. The slope depends on the hydrodynamic radius of both the protein and PEG molecules, with more negative slopes and higher precipitation effectiveness and higher precipitation effectiveness and impact on solution viscosity.

Figure 3a,c shows the solubility of mAb-1 and mAb-2 versus PEG concentration. At all three titers, mAb-1 did not precipitate until the PEG concentration exceeded 20 wt/vol%. No higher PEG concentrations were investigated because they would be impractical for use and irrelevant to the combined PEG/ZnCl₂ precipitation method. The solubility of mAb-1 is well above 51 g/L at PEG concentrations below 20 wt/vol%. In addition, the intrinsic solubility of mAb-1 in pH 7 HEPES buffer is greater than 102 g/L, its concentration prior to the twofold dilution in our precipitation protocol, and no turbidity was observed. The data point for 51 g/L mAb-1 at 25 wt/vol% PEG is

TABLE 1 mAb titers and precipitant concentration ranges

	mAb-1	mAb-2
Titers (g/L)	2.75	2.86
	5.50	5.73
	51.0	29.0
PEG-3350 (wt/vol%)	0 - 25	0 - 25
ZnCl ₂ (mM)	0 - 50	0 - 5 (DS), 0 - 20 (HCCF)

Abbreviations: DS, drug substance; HCCF, harvested cell culture fluid; mAb, monoclonal antibody; PEG, polyethylene glycol.

missing because a nonflowing gel formed that did not settle by centrifugation and could not be dewatered with 0.2 μ m centrifugal filters.

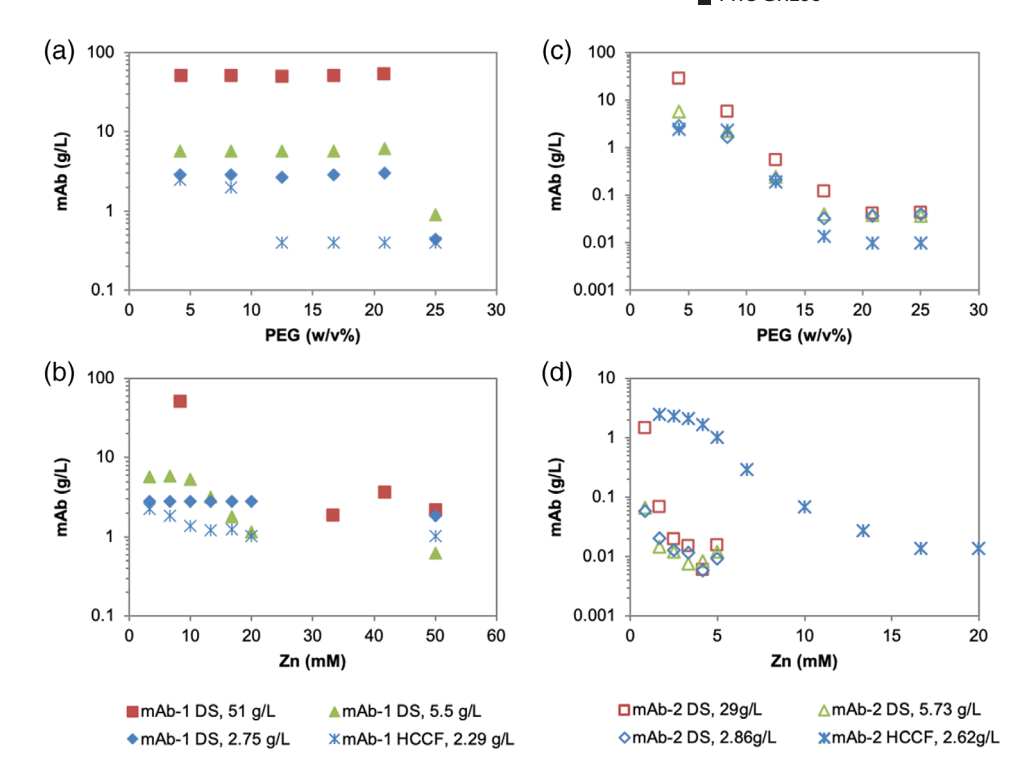
mAb-2 was much less soluble and exhibited the classic log-linear solubility behavior with respect to PEG concentration as illustrated in Figure 3c. More than 50% of the mAb-2 was precipitated by 8.33 wt/vol% PEG for all three titers and at 8.33 wt/vol% PEG, the solubility was less than 0.1 g/L in each case. Based on the 29 g/L titer data, the extrapolated mAb-2 intrinsic solubility is 135 g/L; this is consistent with the observation that the initial 58 g/L mAb-2 solution prior to twofold dilution during precipitation was stable and free of precipitates.

The mechanism for $ZnCl_2$ protein precipitation is not as well established in the literature. The hypothesis is that hydrated $Zn^{2+}_{(aq)}$ species crosslink surface accessible ligands on the protein by forming coordination complexes in a ligand exchange process. Protein-supplied ligands include nitrogen, oxygen, and sulfur electron donors from histidine, glutamate, aspartate, and cysteine side chains, as well as the N-terminus. A complicating factor is that $Zn^{2+}_{(aq)}$ binding increases the net charge of the protein and alters the surface distribution of charged groups.

mAb-1 had complex solubility behavior in ZnCl₂ solutions as shown in Figure 3b. No precipitation was observed at the lowest titer, 2.75 g/L, over the initial 3.33-20 mM ZnCl₂ range, so a data point at 50 mM ZnCl₂ was added and a slight reduction in solubility was found. For the medium titer, 5.5 g/L, 20 and 50 mM ZnCl₂ yielded 79 and 89% precipitation, respectively. For the highest titer, 51 g/L, many data points between 8.3 and 33.3 mM are missing due to the formation of a nonsettleable, nonfilterable turbid phase. This nonsettling behavior has been reported by Sauter et al³⁴ and Zhang et al³⁵ as part of reentrant condensation phase behavior. They found that protein in solution forms a turbid mixture when selected multivalent metal ions are added above a critical concentration C*, but that the supernatant solution becomes clear again above a higher concentration C**. They also found that it took extended periods of time (many hours to days) for solutions in the turbid, two-phase regime to clarify: β-lactoglobulin and ZnCl₂ solutions near (pseudo-)C** formed crystals within 24 hr³⁴ while turbid bovine serum albumin and YCl₃ solutions eventually precipitated after days.³⁵ In our study, the missing points at 51 g/L mAb-1 for intermediate ZnCl2 concentrations would fall in the two-phase region on the phase diagram, though the samples did not clarify after 24 hr. A distinct precipitate phase was formed at 50 mM ZnCl₂, giving a solubility of 2.2 g/L. At the two highest ZnCl₂ concentrations for the 51 g/L case, protein crystals formed at the bottom of the tube while precipitate floated at the top.

On the other hand, $ZnCl_2$ precipitation was uniformly effective for mAb-2. At all three titers, $ZnCl_2$ concentrations greater than 2 mM reduced the solubility to about 0.01 g/L, representing precipitation yields greater than 99% for all cases as shown in Figure 3d. The relative effectiveness of $ZnCl_2$ with mAb-2 at low concentrations compared with mAb-1 might be explained by their difference in pl, which hints at differences in numbers of surface-available cross-linking ligands. In addition, mAb-2 was known to be prone to aggregation. Unlike mAb-1, there was no formation of a nonflowing gel or crystals for mAb-2 precipitation at intermediate concentrations.

FIGURE 3 Batch solubility of mAb-1 and mAb-2 in DS form in 50 mM pH 7.0 HEPES buffer and in HCCF form against PEG-3350 and ZnCl₂, respectively. mAb-1: (a,b), mAb-2: (c,d). Standard deviations for solubility measurements were estimated as 0.1, 0.2, and 1.4 g/L for mAb-1 at 2.75 g/L, 5.5 g/L and 51 g/L, respectively, from data in (a) for PEG concentrations less than 20 wt/vol%, where no precipitation occurred. DS, drug substance; HCCF, harvested cell culture fluid: mAb, monoclonal antibody; PEG, polyethylene glycol



From the solubility data obtained with the two mAbs at the three titers studied, the concentration ranges for PEG and ZnCl₂ were chosen as 0–25 wt/vol% and 0–20 mM, respectively, for the next stage of precipitation screening.

3.2 | Batch precipitation of mAb in HCCF

Figure 3a,b shows the solubility behavior of mAb-1 in HCCF compared with mAb-1 in DS pool form in HEPES buffer. For this stage, the mAb-1 HCCF was concentrated so that the titer during precipitation, 2.29 g/L, would be similar to the 2.75 g/L used in DS form. Unexpectedly, the same concentrations of PEG or ZnCl $_2$ resulted in significantly more precipitation and lower solubility for mAb-1 in HCCF versus the DS form. It may be that the higher pH of the mAb-1 HCCF, 7.5, relative to the HEPES buffer used with mAb-1 in DS form (pH 7), shifted the net charge closer to its pl and reduced its intrinsic solubility in the case of PEG precipitation, and perhaps also titrated surface His residues such that Zn $^{2+}_{\rm (aq)}$ binding was more extensive or effective in the case of zinc precipitation. We note that zinc ion speciation in solution is a function of pH, with the formation of hydroxychloride complexes becoming significant at pH above 7.5, 32 and that this may impact cross-linking effectiveness as well.

Figure 3c,d shows the solubility of mAb-2 in HCCF compared with that in DS form in HEPES buffer. The original titer of mAb-2 HCCF was 1.38 g/L and it had a pH of 8.0. This solution was concentrated to 18.7 g/L and then diluted using 50 mM HEPES, pH 7.0 buffer to give 2.62 g/L during precipitation, similar to the 2.86 g/L used in DS form. Because the dilution with HEPES buffer shifted the

pH closer to 7, the intrinsic and PEG-dependent solubilities of mAb-2 in the treated HCCF and DS forms were expected to be similar as was observed. However, $ZnCl_2$ precipitation of mAb-2 in HCCF required much higher concentrations to achieve solubilities comparable to those in DS form. A possible explanation is that impurities in the mAb-2 HCCF might bind with $Zn^{2+}_{(aq)}$ species and act as depletants. This behavior was markedly different from that of mAb-1 HCCF, possibly due to differences in their impurity profiles.

Given the increased effectiveness of the individual precipitants with mAb-1 HCCF, upper concentration limits of 12.5 wt/vol% PEG and 10 mM $\rm ZnCl_2$ were used for batch precipitations with the combined precipitants. Figure 4a shows the solubility behavior of mAb-1 in HCCF with the dashed curve indicating 95% precipitation yield at the 2.29 g/L titer. The roughly linear nature of the boundaries between the colored zones of the solubility heat maps and of the 95% yield isotherm suggests that the solubility reduction effects of PEG and $\rm ZnCl_2$ are approximately additive.

For mAb-2 HCCF precipitations, 12.5 wt/vol% PEG and 4 mM $ZnCl_2$ were chosen as the upper concentration limits with solubility results shown in Figure 4b along with the 95% yield curve at the 3.02 g/L titer. Note that a new batch of HEPES-diluted mAb-2 HCCF was prepared from the 18.7 g/L stock solution for this screen. Again, the solubility-reducing effects of the precipitants were approximately additive for mAb-2 in treated HCCF.

The data in Figure 4 suggest, as a first approximation, an empirical expression for protein solubility, *S*, for the PEG/ZnCl₂ system that is an additive function of precipitant concentration,

$$ln(S) = \beta - K_{PEG}[PEG] - K_{Zn}[ZnCl_2], \tag{4}$$

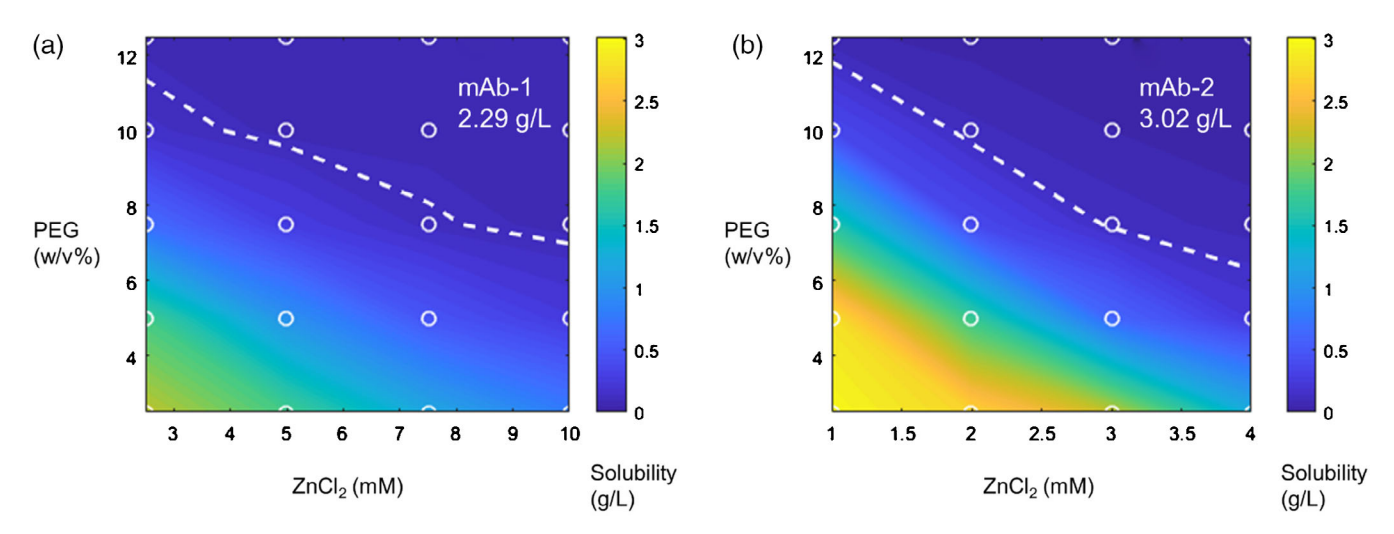


FIGURE 4 Batch solubility map of mAb-1 in HCCF at 2.29 g/L (a) and mAb-2 in treated HCCF at 3.02 g/L (b). The open circles indicate the conditions where solubility measurements were made. The dashed lines indicate a solubility of 0.11 g/L and 0.15 g/L, for (a) and (b), respectively, representing 95% precipitation yield isotherms for these titers. Note that the scales for the $ZnCl_2$ concentration axes on the two plots are different, reflecting the greater effectiveness of $ZnCl_2$ as a precipitant for mAb-2. HCCF, harvested cell culture fluid; mAb, monoclonal antibody; PEG, polyethylene glycol

where β is a value that incorporates the protein intrinsic solubility as well as the impact of protein-protein interactions in solution, which decrease in solutions with low solubility; [PEG] and [ZnCl₂] are the concentrations of the precipitants; and K_{PEG} and K_{Zn} are the sensitivities of the solubility to the precipitants, analogous to the salting-out constant in the Cohn-Setschenow equation for salt-induced precipitation. The log-linear solubility reduction relationship in PEG concentration in Equation (1) has a good basis in the excluded volume precipitation mechanism while that for the ZnCl₂ concentration is a simplification without regard to the more complex binding and cross-linking precipitation mechanism of divalent transition metal ions. The 95% precipitate yield isotherms correspond to plots of

yield =
$$95\% = \frac{P_o - S}{P_o}$$
 (5)

which reflects the solubility required to meet the specified yield for a given initial protein concentration, P_o . Equations (4) and (5) provide a convenient rubric for the interpretation and comparison of the solubility maps.

Examining the HCCF solubility behaviors shown in Figure 4, mAb-1 and mAb-2 are similar in their response to PEG concentration implying $K_{\text{PEG, mAb1}} \sim K_{\text{PEG, mAb2}}$, while mAb-2 is much more sensitive to ZnCl₂ concentration, with $K_{\text{Zn, mAb1}} < K_{\text{Zn, mAb2}}$. The similarity in PEG effectiveness is expected given the dependence on mAb molecular volume; this is also mirrored by the similarity of the slopes of the DS solubility curves in Figure 3a,c. There is, however, a constant offset in the solubility that may reflect differences in the intrinsic solubilities of the antibodies, suggesting $\beta_{\text{mAb1}} < \beta_{\text{mAb2}}$. This offset may arise from differences in surface chemistry, given the different pl and 0.5 unit difference in the pH of the HCCF. For ZnCl₂ precipitation, where ion binding by target and contaminant species determines behavior,

the combination of differences in mAb surface chemistry, solution pH, and impurity profiles resulted in significant differences in both the effectiveness of $ZnCl_2$ as a precipitant as well as in the absolute amount of $ZnCl_2$ needed to generate precipitates at similar titers. This is echoed in the solubility data for the antibodies in DS form as shown in Figure 3b.d.

Curvature in the boundaries between the colored zones of the solubility heat maps and in 95% yield isotherm, and convex downward behavior in particular, is indicative of synergistic action between PEG and ${\rm Zn^{2+}}_{\rm (aq)}$. Some convex downward curvature is apparent in the solubility behavior of mAb-2 with increasing ZnCl₂ concentration, as shown in Figure 4b. Synergy is not unexpected as the addition of PEG will increase the thermodynamic activity of all species in solution and ${\rm Zn^{2+}}_{\rm (aq)}$ cross-linking of monomers will increase the excluded volume of the mAb.

3.3 | Effect of mAb-2 HCCF conditioning on solubility

Given that the mAb-2 HCCF was conditioned by microfiltration and dilution with a lower pH HEPES buffer, we further explored the impact of the solution used for dilution on mAb-2 solubility behavior. Three solutions were investigated: 50 mM HEPES, pH 7 buffer; the pH 8 filtrate obtained from the mAb-2 concentration step; and the filtrate pH-adjusted to 7 using HCl. For these measurements, a 22.8 g/L mAb-2 HCCF stock solution was used and diluted to 6 g/L prior to precipitation. The resulting PEG and ZnCl₂ solubility data are shown in Figure 5. Note that when HEPES buffer was used to dilute the HCCF, the mAb concentration in some supernatants was below the 0.0101 g/L detection limit of the Cedex BioHT analyzer; in these instances, 0.0101 g/L was used as an upper bound on the solubility.

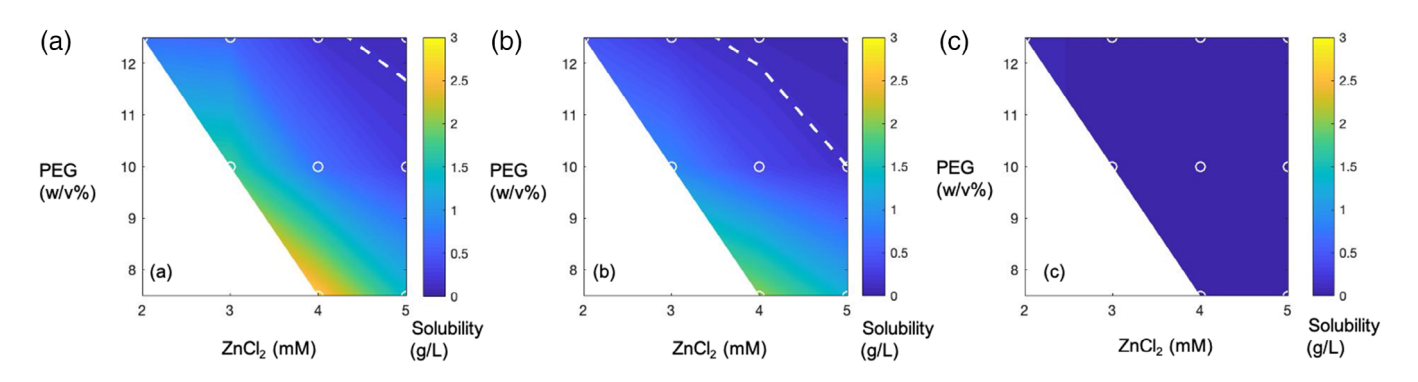


FIGURE 5 Batch solubility map of mAb-2 in HCCF at 3.0 g/L, conditioned by concentration and dilution with three different solutions: (a) filtrate at pH 8.0, (b) filtrate pH-adjusted to 7.0, (c) 50 mM HEPES buffer at pH 7.0. The open circles indicate the conditions where solubility measurements were made. The blank regions at lower precipitant concentrations were not examined in this screen. Dashed lines indicate a solubility of 0.15 g/L, representing a 95% precipitation yield at this titer. HCCF, harvested cell culture fluid; mAb, monoclonal antibody

Both the pH of the HCCF and the impurity profile play a significant role in mAb-2 solubility behavior. All solubilities at comparable PEG and ZnCl₂ concentrations decreased in the order: pH 8 filtrate > pH 7 filtrate > pH 7 HEPES buffer. Comparison of Figure 5a,b indicates that mAb-2 is generally more soluble at pH 8 than pH 7, suggesting that $\beta_{\rm mAb2,\ pH7}$ < $\beta_{\rm mAb2,\ pH8}$, while the sensitivities to PEG and ZnCl₂, indicated by the values of K_{PEG} and K_{ZnCl2} , were similar. Comparison of Figure 5b,c indicates that dilution with HEPES buffer rather than with pH-adjusted filtrate results in a significant, across-the-board decrease in solubility corresponding to the decreased levels of impurities. Assuming the original mAb-2 HCCF has a mAb: "small" (nominally <30 kDa) impurities ratio of 1:1, after a 15-fold concentration using SPTFF and dilution to 6 g/L with HEPES buffer prior to precipitation, this ratio becomes 4:0.26: after concentration and dilution to 6 g/L with filtrate the ratio becomes 4:1 for both the pH 8 and pH 7 cases. We attribute the HEPES dilution effect to increased effective concentrations of ZnCl₂ at lower absolute impurity concentrations, manifested as increased sensitivity, that is, $K_{Zn, buffer} > K_{Zn, filtrate}$; proteinaceous impurities and DNA fragments as well as any residual chelators from the growth media are presumed to deplete Zn²⁺(aq) species. This suggests incorporation of a HCCF conditioning step prior to precipitation may be beneficial. Dilutions with both pH-adjusted filtrate and HEPES buffer were carried over into the HTP screening stage to further explore the differences in solubility behavior.

3.4 | HTP precipitation of mAbs in HCCF

HTP precipitation and redissolution screening of the two mAbs in HCCF were performed on a Tecan Evo2 liquid handling robot. For each mAb, two titers were selected to represent current, 2.5–3 g/L range, and future, 8–15 g/L range, upstream process titers. The highest concentrations for PEG and ZnCl $_2$ in the HTP experiments were set to 12.5 wt/vol% and 25 mM, respectively. For mAb-2 HCCF diluted with HEPES buffer, the maximum ZnCl $_2$ concentration was reduced to 7 mM, given the greater effectiveness of ZnCl $_2$ for this conditioning approach.

For the current upstream process titer case, HCCF was used as is. The resulting titers after twofold dilution during precipitation were 1.41 g/L for mAb-1 and 1.24 g/L for mAb-2. The solubility maps comparing mAb-1 and mAb-2 for this case are shown in Figure 6a,c. Note that PEG concentrations greater than 8–10 wt/vol% and ZnCl $_2$ concentrations greater than 15 mM are required to achieve the $\sim\!0.06$ mg/ml solubilities that give antibody yields of 95% in the precipitate phase. This makes sense, as this was the lowest titer case studied. Given supernatant concentration measurement error at these low solubilities, the behaviors of the two antibodies in the current titer case are similar.

Pairwise comparisons of the solubility data of the current and future HCCF titer cases are represented by Figure 6a,b for mAb-1 and by Figure 6c.d for mAb-2. The future titer case for mAb-1 was prepared by concentration, giving 7.47 g/L during precipitation. Assuming a mAb-1:small impurity ratio of 1:1 for the current titer case, the future titer case had a ratio of \sim 5.3:1. The future titer case for mAb-2 was prepared by 15-fold concentration and dilution with filtrate to 4.10 g/L during precipitation. Similarly, assuming a mAb-2:small impurity ratio of 1:1 for the current titer case, the future titer case had a ratio of ~5.5:1. As expected, the concentrations of PEG and ZnCl₂ needed to achieve solubilities found for the current titer case were similar to the future titer case and the 95% yield isotherms shifted to lower precipitant concentrations. The similar solubilities were expected as changes in titer should not change the parameters in the solubility relationship suggested in Equation (4), as long as the crosslinking Zn²⁺_(aq) species are present in comparable stoichiometric excess with respect to mAb and impurity levels both the cases. As titer increases, the absolute solubility required to achieve a 95% yield increases per Equation (5), meaning that lower concentrations of precipitant are needed. Assuming that typical Zn²⁺_(aq) dissociation constants for coordination of side-chain ligands are $\sim\!\!1\,\text{mM}^{32}$ and that there are roughly 10 Zn²⁺_(ao) binding sites per mAb, with only a subset of these sites accessible for cross-linking, and also taking into account the range of mAb titers examined was 20–100 $\mu M,$ target binding and precipitation should not significantly deplete the supply of Zn²⁺(aq) available over the multimillimolar ZnCl2 concentration ranges studied.

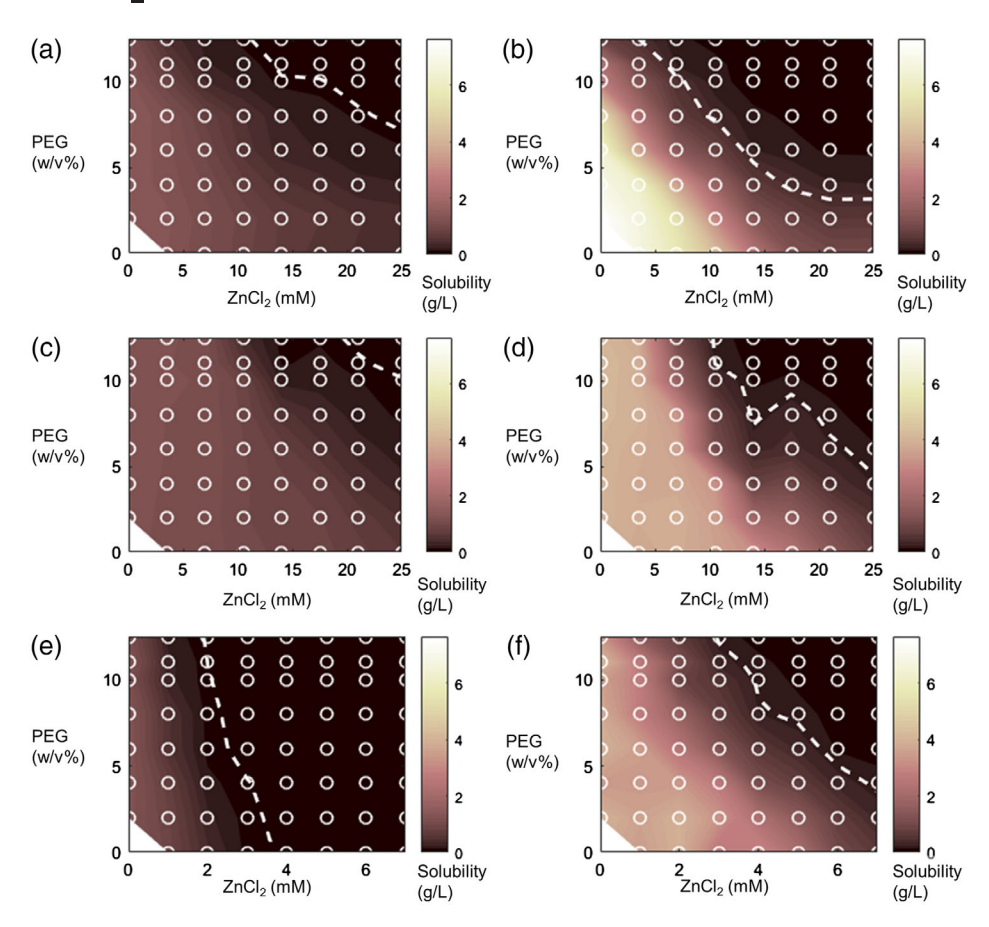


FIGURE 6 High throughput precipitation solubility maps of mAb-1 HCCF at (a) 1.41 g/L and (b) 7.47 g/L, and mAb-2 HCCF diluted with filtrate to (c) 1.24 g/L and (d) 4.10 g/L and mAb-2 diluted with pH 7 HEPES buffer to (e) 1.15 g/L and (f) 3.98 g/L. The open circles indicate the conditions where solubility measurements were made. The blank regions near the origin indicate where the solubility exceeded the titer. Dashed lines represent 95% precipitation yields for the titers used on each solubility map. Note that the scales for the ZnCl₂ concentration axes in (e) and (f) differ from the others, reflecting the greater effectiveness of ZnCl₂ as a precipitant for mAb-2 HCCF diluted with HEPES buffer. HCCF, harvested cell culture fluid; mAb, monoclonal antibody

The presence of more cross-linkable protein molecules at higher titers simply enables more cross-linking and precipitation to occur at a given ZnCl₂ concentration.

To follow up on the effects of HCCF conditioning on mAb-2 solubility behavior, HEPES buffer was also used to dilute the concentrated mAb-2 HCCF stock solution to match the current and future HCCF titer cases, giving mAb-2:small impurity ratios of 0.77:0.05 and 5.31:0.35, respectively. The corresponding solubility behaviors are shown in Figure 6c,e for the current titer case and Figure 6d,f for the future titer case. For both cases, ZnCl₂ was significantly more effective when the absolute concentrations of small impurities were depleted by dilution with HEPES buffer rather than filtrate, again suggesting $K_{Zn, filtrate} < K_{Zn, buffer}$. Curiously, there was some dependence of solubility on mAb-2 titer when dilutions were completed with HEPES buffer as shown in Figure 6e,f. The current titer case was generally less soluble than the future titer case in this HCCF conditioning approach; this is shown clearly by the shift in the 95% yield isotherm to lower precipitant concentrations for the current titer case relative to the future titer case. This is another indication that the roughly sevenfold lower relative concentration of small impurities in the current titer case versus the high titer case resulted in greater sensitivity to ZnCl₂ concentration. If PEG/ZnCl₂ precipitation were to be used to purify mAb-2, the addition of a HCCF preconditioning step, such as ultrafiltration/diafiltration or dilution with buffer immediately before the precipitation step might be advantageous.

The overall solubility behaviors of all the systems shown in Figure 6 were still roughly additive in PEG and ZnCl₂ concentration. There is some evidence for precipitant synergy for mAb-1 at higher ZnCl₂ concentrations.

3.5 Product quality after redissolution

Precipitation takes advantage of the aggregation and clustering of protein molecules. Given the potential for activity losses and immunogenicity when therapeutic proteins aggregate, 38 it is important to consider the redissolution behavior of precipitates when performing target species precipitation. The precipitants chosen here, PEG and ZnCl₂, generate reversible protein precipitates with facile redissolution of pelleted material by dilution with neat buffer in the case of PEG³⁹ and by acidification of the solution in the case of Zn² +(ao). 20,33 All dewatered precipitate phases examined in this work were completely dissolved by resuspension using 1,000 µl of 100 mM acetate buffer, pH 5.0; no residual particulate matter or turbidity were observed.

In order to verify the antibody quality with respect to high molecular weight impurities (HMWI) and low molecular weight impurities (LMWI) after precipitation and redissolution, samples from the second stage manual batch precipitations with greater than 95% yield for mAb-1 HCCF were assayed via SEC. These results were compared against mAb-1 samples obtained after a typical protein A purification

TABLE 3 SEC results of batch precipitated and redissolved mAb-2 in HCCF at 5.0 g/L after mixing for precipitation. In all cases, precipitate yield exceeded 98.4% based on the mAb supernatant detection limit of 0.08 g/L

TABLE 2	SEC results for impurities in batch precipitated and		
redissolved r	nAb-1 in HCCF at 2.29 g/L during precipitation. With		
one exception, precipitate yield exceeded 96.5% based on the mAb			
supernatant	detection limit of 0.08 g/L. For the 7.5 mM ZnCl ₂ and		
7.5 wt/vol%	PEG case, the precipitate yield was 94.5%		

Zn (mM)	PEG (wt/vol%)	% HMW	% Monomer	% LMW
7.5	7.5	1.74	92.45	5.80
10.0	7.5	1.80	92.77	5.43
5.0	10	1.88	92.59	5.53
7.5	10	1.78	91.92	6.30
10.0	10	1.66	92.45	5.89
2.5	12.5	2.16	93.49	4.35
5.0	12.5	1.84	92.01	6.15
7.5	12.5	1.65	91.10	7.25
10.0	12.5	1.58	91.61	6.81
Protein A		3.73	96.11	0.17

Abbreviations: HCCF, harvested cell culture fluid; HMW, high molecular weight; LMW, low molecular weight; mAb, monoclonal antibody; PEG, polyethylene glycol; SEC, size exclusion chromatography.

step used in pilot plant operations in-house. Table 2 shows the HMWI and LMWI percentages at a titer of 2.29 g/L post redissolution as a function of the concentration of PEG and ZnCl₂ used in the precipitation. The most obvious characteristic is that the precipitated and redissolved samples contain much more LMWI than the average value of post-protein A samples. Protein A does not bind to LMWI species that lack Fc regions while LMWI may be coprecipitated with mAb monomer.

On a LMWI-free basis, mAb-1 monomer constitutes about 97% and HMWI 3% of the redissolved precipitate, which is comparable to that of the post-protein A samples. Thus, PEG/ZnCl₂ precipitation and redissolution did not increase the proportion of HMWI species in mAb-1. This finding is consistent with prior work in our lab precipitating bovine serum albumin with PEG and ZnCl₂ (unpublished results), where circular dichroism and SEC analyses of redissolved precipitate suggested that PEG/ZnCl₂ precipitation induced no significant monomer secondary structural change nor aggregation of this aggregation-prone protein.

Several strategies could be used to clear LMWI in a precipitation process. In addition to boosting precipitation performance, conditioning HCCF by preconcentration would remove LMWI. Further, incorporation of dewatering and washing steps between precipitation and redissolution may remove LMWI to further improve monomer purity. In our related continuous precipitation process study with mAb-1, 29 a microfiltration-based countercurrent precipitate washing operation was incorporated to remove impurities, including host cell proteins, HMWI, and LMWI. In addition, as the precipitate yield increases with increasing PEG and ZnCl2 concentrations, the monomer purity decreases demonstrating a tradeoff between product purity and yield at fixed titer.

For completeness, and despite the lack of availability of in-house data for protein A purification performance, we conducted a similar

Zn (mM)	PEG (wt/vol%)	% HMW	% Monomer	% LMW
6	10	50.22	40.91	8.87
6	11	49.30	41.57	9.13
6	12.5	48.15	42.74	9.11
7	8	61.16	30.03	8.81
7	10	54.44	36.31	9.26
7	11	43.32	47.46	9.22
7	12.5	35.61	53.66	10.74

Abbreviations: HCCF, harvested cell culture fluid; HMW, high molecular weight; LMW, low molecular weight; mAb, monoclonal antibody; PEG, polyethylene glycol; SEC, size exclusion chromatography.

SEC analysis of redissolved mAb-2 quality after precipitation from HCCF conditioned by dilution to a titer of 5.0 g/L using HEPES buffer; the results are given in Table 3. In all cases, HMWI levels for mAb-2 were extreme. After redissolution, the purity of the mAb-2 solutions were estimated to be between 30 and 50%, with about 10% LMWI and the remaining 40-60% of HMWI. A confounding variable in this case was that due to competing process analytical priorities, the mAb-2 samples were stored in a -80°C freezer for about 2 months after redissolution and before analysis, which might have contributed to the observed aggregation or degradation behavior; mAb-1 samples were similarly stored in a -80°C freezer but for a period of only 2-3 weeks. It was confirmed with the manufacturer that mAb-2 is prone to aggregation. Therefore, additional precipitation experiments using PEG and ZnCl₂ are needed to confirm the results for mAb-2. If the low monomer purity is confirmed, pursuit of PEG/ZnCl₂ precipitation for mAb-2 would not be fruitful.

4 | CONCLUSIONS

The PEG and ZnCl₂ solubility and precipitate redissolution behaviors of two commercially relevant mAbs were investigated in DS form in HEPES buffer and in HCCF form using manual and HTP screening formats. The objective was to determine the appropriate solution conditions for solubility reduction resulting in high precipitation yield and good quality on redissolution for further study in a continuous tubular precipitation reactor at laboratory scale.

The manual batch precipitations with DS and HCCF allowed us to scope out the relevant PEG and ZnCl₂ concentration ranges for mAb-1 and mAb2 for several titers. The solubility of both mAbs was found to be a roughly additive function of the concentrations of PEG and ZnCl₂ precipitants and a basic empirical solubility relationship was proposed to serve as a framework for the interpretation of the results. Both mAbs behaved similarly with respect to PEG concentration, while mAb-2 was more sensitive to ZnCl₂ concentration. mAb-2 solubility was reduced as pH decreased from 8 to 7, presumably by

moving closer to the pl. HCCF titer had little impact on solubility behavior, excepting those cases where conditioning led to reductions in the relative amounts of LMWI and $ZnCl_2$ and precipitant effectiveness was enhanced. It was presumed that low molecular weight species exerted their effect by the competitive binding of $Zn^{2+}_{(aq)}$ species.

Select conditions with high precipitation yields for both mAbs were repeated, and redissolved mAbs were analyzed for product quality in terms of the presence of HMWI and LMWI species. It was found that redissolved mAb-1 contained more LMWI than typical of protein A-processed mAb-1. The relative proportions of monomer and HMWI species were similar to, and perhaps even slightly less than that typical of post-protein A mAb-1 samples. On the other hand, redissolved mAb-2 showed extensive HMWI content, likely due to its innate tendency to aggregate and possibly aggravated by long-term storage in a –80°C freezer prior to analysis.

The aggregation and precipitation behaviors of mAb-1 and mAb-2 offer an interesting contrast. For a well-behaved antibody like mAb-1, precipitates may be based on aggregates that are biophysically distinct from "stability aggregates." Stability aggregates may be reversibly incorporated into precipitate particles without driving formation of additional stability aggregate. For an aggregation-prone antibody like mAb-2, the promotion of protein-protein interactions by precipitation may exacerbate the formation of stability aggregates.

On the HTP platform, two titers of both mAbs were investigated to represent current and future upstream bioprocess productivity. For mAb-1, selected conditions were further investigated using a continuous precipitation reactor with a countercurrent multistage precipitate washing step using microfiltration and results are presented in another publication.²⁹ For mAb-2, it was found that the conditioning of the HCCF could affect the solubility and precipitation yield. Two diluents, pH 7 HEPES buffer and filtrate obtained from concentrating HCCF, were used to dilute preconcentrated HCCF to enable exploration of titer effects. It was found and confirmed that the absolute amount of LMWI had a significant impact on the effectiveness of ZnCl₂ as a precipitant for mAb-2. HCCF conditioning in terms of titer, pH, and impurity profile adjustment is an additional operational lever that can be manipulated to control target precipitation performance.

The use of multiple precipitants in combination has several advantages. Additivity in solubility reduction power is helpful as it permits, in the case of the PEG/ZnCl₂ system, solution viscosity to be manipulated independently from target protein solubility which may reduce the burden on subsequent steps required to remove residual precipitants. We note that where significant synergy in precipitating effectiveness exists, it would have great benefits in terms of reduced precipitant usage, reducing footprint, resources, and cost in purification processes. Synergy was observed at higher ZnCl₂ concentrations for both mAbs.

The HTP platform is especially valuable for investigating precipitation and redissolution. Here concentrations of two precipitation reagents, PEG and $ZnCl_2$, were systematically varied to locate the optimal conditions for higher precipitation yield of two mAbs. The number of PEG/ $ZnCl_2$ combinations examined at one time was 64,

TABLE 4 Summary of mAb-1 HCCF precipitation conditions and solubility behaviors across three platforms. mAb-1 HCCF conditioned by concentration of the original culture fluids in each case

	Batch	High throughput		Continuous
mAb-1 titer (g/L)	2.29	7.47	1.41	2.3
PEG (wt/vol%)	7.5	8	8	7
ZnCl ₂ (mM)	10	10.5	10.5	10
Residence time	4 hr	2 hr	2 hr	30 s
Observed solubility (g/L)	0.07	0.04	0.49	80.0
Precipitation step yield	97%	95%	65%	97%
Washing step yield	_	_	_	82%
Overall yield	-	_	_	80%

Abbreviation: HCCF, harvested cell culture fluid; mAb, monoclonal antibody; PEG, polyethylene glycol.

including a negative control (no PEG or $ZnCl_2$), where each condition required only 500 μ l of mAb HCCF. For HTP experiments at a final mAb titer of 1 g/L, the total amount of mAb needed per plate was only 0.064 g. Thus, 1 g of mAb is enough to study 1,000 different conditions. On the other hand, with the development of HTP liquid handling platforms, analytical methods need to be adapted into the HTP format. Routine tests, such as SEC, CHO-HCP, and DNA assays have different advantages and difficulties when implemented with HTP. There is specialized equipment for HTP analytics commercially available, but access to these techniques is still a bottleneck. Overall, the use of an HTP platform can increase the efficiency of process development and optimization and can accelerate the commercialization of a drug product.

This solubility study was run in parallel with a study of a lab-scale process which integrated target precipitation, precipitate dewatering, precipitate washing, and redissolution steps in a continuous operation using mAb-1. Initial results for the optimal precipitant concentrations were selected²⁹ based on studies of the precipitation of mAb-1 in three different platforms: batch, HTP, and continuous reactor. Table 4 compares the mAb titer, precipitation conditions, precipitation step yield, and overall yields obtained in this work with those from a 1-hour run of the continuous process.²⁹ We note that the batch screening experiments and the continuous precipitation run used the same lot of mAb-1 HCCF.

From Table 4 we can conclude that the results from the batch and continuous formats are consistent and transferrable with the $PEG/ZnCl_2$ precipitation system. In addition, the HTP format identified similar conditions that could result in a 95% precipitation yield for a stream with three times the titer of the original HCCF indicating ready adaptability to increasing titers. Low titer streams may not have sufficient concentration for significant precipitation due to low levels of cross-linking and reduced total excluded volumes. What is more exciting is the reduced residence time from batch to HTP to continuous format, emphasizing the potential improvement of efficiency by using HTP in process development to achieve effective HTP processes by continuous precipitation.

ACKNOWLEDGMENTS

This work was supported by NSF-GOALI grant No. CBET1705642. QG was also supported by the Carnegie Mellon University Department of Chemical Engineering and a PPG Fellowship. Thanks to Christopher Inong for help with writing Tecan scripts, and Matt Brown and Dr. Raquel Orozco from BI for insightful discussions.

ORCID

Todd M. Przybycien https://orcid.org/0000-0003-0111-3640 Andrew L. Zydney https://orcid.org/0000-0003-1865-9156

REFERENCES

- Shukla AA, Wolfe LS, Mostafa SS, Norman C. Evolving trends in mAb production processes. *Bioeng Transl Med.* 2017;2(1):58-69. https://doi.org/10.1002/btm2.10061.
- Somasundaram B, Pleitt K, Shave E, Baker K, Lua LHL. Progression of continuous downstream processing of monoclonal antibodies: current trends and challenges. *Biotechnol Bioeng*. 2018;115(12):2893-2907. https://doi.org/10.1002/bit.26812.
- Farid SS. Process economics of industrial monoclonal antibody manufacture. J Chromatogr B. 2007;848(1):8-18. https://doi.org/10.1016/j.jchromb.2006.07.037.
- Girard V, Hilbold NJ, Ng CKS, et al. Large-scale monoclonal antibody purification by continuous chromatography, from process design to scale-up. *J Biotechnol*. 2015;213:65-73. https://doi.org/10.1016/j. jbiotec.2015.04.026.
- Natarajan V, Zydney AL. Protein a chromatography at high titers. Biotechnol Bioeng. 2013;110:2445-2451. https://doi.org/10.1002/bit. 24902.
- Anderson NL, Anderson NG. The human plasma proteome: history, character, and diagnostic prospects. Mol Cell Proteomics. 2002;1(11): 845-867. https://doi.org/10.1074/mcp.R200007-MCP200.
- Bertolini J. In: Simon TL, McCullough J, Snyder EL, Solheim BG, Strauss RG, eds. Rossi's Principles of Transfusion Medicine. Hoboken, NJ, USA: John Wiley & Sons, Ltd; 2016:302-320. https://doi.org/10. 1002/9781119013020.ch27.
- Thömmes J, Etzel M. Alternatives to chromatographic separations. Biotechnol Prog. 2007;23:42-45. https://doi.org/10.1021/bp0603661.
- Swartz AR, Sun Q, Chen W. Ligand-induced cross-linking of Z-elastinlike polypeptide-functionalized E2 protein nanoparticles for enhanced affinity precipitation of antibodies. *Biomacromolecules*. 2017;18(5): 1654-1659. https://doi.org/10.1021/acs.biomac.7b00275.
- Kateja N, Kumar D, Sethi S, Rathore AS. Non-protein a purification platform for continuous processing of monoclonal antibody therapeutics. J Chromatogr A. 2018;1579:60-72. https://doi.org/10.1016/j. chroma.2018.10.031.
- Zydney AL. Continuous downstream processing for high value biological products: a review. *Biotechnol Bioeng*. 2015;113(3):465-475. https://doi.org/10.1002/bit.25695.
- Hammerschmidt N, Hobiger S, Jungbauer A. Continuous polyethylene glycol precipitation of recombinant antibodies: sequential precipitation and resolubilization. *Process Biochem.* 2016;51:325-332. https:// doi.org/10.1016/j.procbio.2015.11.032.
- Hekmat D. Large-scale crystallization of proteins for purification and formulation. *Bioprocess Biosyst Eng.* 2015;38:1209-1231. https://doi. org/10.1007/s00449-015-1374-y.
- Rosa PAJ, Azevedo AM, Sommerfeld S, Mutter M, Bäcker W, Aires-Barros MR. Continuous purification of antibodies from cell culture supernatant with aqueous two-phase systems: from concept to process. *Biotechnol J.* 2013;8(3):352-362. https://doi.org/10.1002/biot. 201200031.

- Bell DJ, Hoare M, Dunnill P. The formation of protein precipitates and their centrifugal recovery. Adv Biochem Eng Biotechnol. 1983;26: 1-72.
- Rothstein F. Differential precipitation of proteins: science and technology. In: Harrison RG, ed. Protein Purification Process Engineering. New York, NY, USA: Marcel Dekkaer, Inc.; 1993:115-208.
- Atha DH, Ingham KC. Mechanism of precipitation of proteins by polyethylene glycols. Analysis in terms of excluded volume. *J Biol Chem*. 1981;256(23):12108-12117.
- Sim SL, He T, Tscheliessnig A, Mueller M, Tan RBH, Jungbauer A. Protein precipitation by polyethylene glycol: a generalized model based on hydrodynamic radius. *J Biotechnol*. 2012;157:315-319. https://doi.org/10.1016/j.jbiotec.2011.09.028.
- Odijk T. Depletion theory and the precipitation of protein by polymer.
 J Phys Chem B. 2009;113:3941-3946. https://doi.org/10.1021/jp806722j.
- Van Dam ME, Wuenschell GE, Arnold FH. Metal affinity precipitation of proteins. *Biotechnol Appl Biochem.* 1989;11(5):492-502.
- 21. Soraruf D, Roosen-runge F, Grimaldo M, et al. Protein cluster formation in aqueous solution in the presence of multivalent metal ions—a light scattering study. *Soft Matter*. 2014;10:894-902. https://doi.org/10.1039/c3sm52447g.
- Li Z, Zydney AL. Effect of zinc chloride and PEG concentrations on the critical flux during tangential flow microfiltration of BSA precipitates. *Biotechnol Prog.* 2017;33(6):1561-1567. https://doi.org/10. 1002/btpr.2545.
- Burgstaller D, Jungbauer A, Satzer P. Continuous integrated antibody precipitation with two-stage tangential flow microfiltration enables constant mass flow. *Biotechnol Bioeng*. 2019;116(5):1053-1065. https://doi.org/10.1002/bit.26922.
- Ahmad SS, Dalby PA. Thermodynamic parameters for salt-induced reversible protein precipitation from automated microscale experiments. *Biotechnol Bioeng*. 2011;108(2):322-332. https://doi.org/10. 1002/bit.22957.
- Dumetz AC, Chockla AM, Kaler EW, Lenhoff AM. Effects of pH on protein-protein interactions and implications for protein phase behavior. *Biochim Biophys Acta*. 2008;1784:600-610. https://doi.org/10. 1016/j.bbapap.2007.12.016.
- Baumgartner K, Galm L, Nötzold J, et al. Determination of protein phase diagrams by microbatch experiments: exploring the influence of precipitants and pH. *Int J Pharm*. 2015;479(1):28-40. https://doi. org/10.1016/j.ijpharm.2014.12.027.
- Knevelman C, Davies J, Allen L, Titchener-Hooker NJ. High-throughput screening techniques for rapid PEG-based precipitation of IgG4 mAb from clarified cell culture supernatant. *Biotechnol Prog.* 2010;26 (3):697-705. https://doi.org/10.1002/btpr.357.
- Shukla AA, Rameez S, Wolfe LS, Oien N, et al. High-Throughput Process Development for Biopharmaceuticals. In: Kiss B, Gottschalk U, Pohlscheidt M, eds. New Bioprocessing Strategies: Development and Manufacturing of Recombinant Antibodies and Proteins. Cham, Switzerland: Springer; 2017:401–441. https://doi.org/10.1007/978-3-319-97110-0.
- Li Z, Gu Q, Coffman JL, Przybycien TM, Zydney AL. Continuous precipitation for monoclonal antibody capture using countercurrent washing by microfiltration. *Biotechnol Prog.* 2019;35(6):e2886. https://doi.org/10.1002/btpr.2886.
- Ferreira CMH, Pinto ISS, Soares EV, Soares HMVM. (Un)suitability of the use of pH buffers in biological, biochemical and environmental studies and their interaction with metal ions-a review. RSC Adv. 2015; 5(39):30989-31003. https://doi.org/10.1039/c4ra15453c.
- Human IgG Assay for Cedex Bio and Bio HT Analyzers. http://www.custombiotech.roche.com/content/dam/internet/dia/custombiotech/custombiotech_com/en_GB/pdf/CustomBiotech_IgG_Assay_for Cedex_Bio_and_Cedex_Bio_HT_Analyzer_ProductFlyer.pdf. Accessed June 10, 2019.

- Krezel A, Maret W. The biological inorganic chemistry of zinc ions. Arch Biochem Biophys. 2016;611:3-19. https://doi.org/10.1016/j.abb. 2016.04.010.
- Arnold FH. Metal-affinity separations: a new dimension in protein processing. *Biotechnology*. 1991;9:151-156. https://doi.org/10.1038/ nbt0291-151.
- Sauter A, Oelker M, Zocher G, Zhang F, Stehle T, Schreiber F. Nonclassical pathways of protein crystallization in the presence of multivalent metal ions. Cryst Growth des. 2014;14(12):6357-6366. https:// doi.org/10.1021/cg501099d.
- Zhang F, Skoda MWA, Jacobs RMJ, et al. Reentrant condensation of proteins in solution induced by multivalent counterions. *Phys Rev Lett.* 2008;101(14):3-6. https://doi.org/10.1103/PhysRevLett.101.148101.
- Setschenow JZ. Uber die konstitution der salzosungenauf grunf auf ihres verhaltens zu kohlensure. Z Phys Chem. 1889;4: 117-125.
- Cohn EJ. The Physical Chemistry of the Proteins. *Physiol. Rev.* 1925;5: 349-437. https://journals.physiology.org/doi/pdf/10.1152/physrev. 1925.5.3.349.

- Ratanji KD, Derrick JP, Dearman RJ, Kimber I. Immunogenicity of therapeutic proteins: influence of aggregation. *J Immunotoxicol*. 2014; 11(2):99-109. https://doi.org/10.3109/1547691X.2013.821564.
- Sim SL, He T, Tscheliessnig A, Mueller M, Tan RBH, Jungbauer A. Branched polyethylene glycol for protein precipitation. *Biotechnol Bioeng*. 2012;109(3):736-746. https://doi.org/10.1002/bit.24343.
- Konstantinidis S, Kong S, Titchener-Hooker N. Identifying analytics for high throughput bioprocess development studies. *Biotechnol Bio*eng. 2013;110(7):1924-1935. https://doi.org/10.1002/bit.24850.

How to cite this article: Gu Q, Li Z, Coffman JL, Przybycien TM, Zydney AL. High throughput solubility and redissolution screening for antibody purification via combined PEG and zinc chloride precipitation. *Biotechnol Progress*. 2020; e3041. https://doi.org/10.1002/btpr.3041